Molecular docking studies of Triphala with catalytic portion of HMG-CoA reductase enzyme

Prasob-Orn Rinthong[iD], **Pawitra Pulbutr**[iD], **Chawannuch Mudjupa***[iD]

Pharmaceutical Chemistry and Natural Product Research Unit, Faculty of Pharmacy, Mahasarakham University, Maha Sarakham, Thailand 44150

A B S T R A C T

Introduction: Triphala, consisting of three fruits, *Phyllanthus emblica* L. (Phyllanthaceae), *Terminalia bellirica* (Gaertn.) Roxb. (Combretaceae), and *T. chebula* Retz, is a well-recognized Ayurvedic herbal formulation, used for various therapeutic purposes, including the treatment of dyslipidemia. Inhibitory activity against 3-hydroxy-3-methylglutaryl-coenzyme A (HMG-CoA) reductase, a rate-limiting enzyme in the endogenous cholesterol synthesis pathway, is an essential target for the management of hypercholesterolemia. This *in silico* study aimed to investigate the HMG-CoA reductase inhibitory activity of the phytochemical compounds derived from Triphala formulation by employing molecular docking analysis.
Methods: Ten phytochemical constituents of Triphala formulation were selectively used for docking study by using the HMG-CoA reductase template (PDB: 1HWK). Docking analysis was performed using AutoDock 4.2. The candidates were ranked by the binding energy parameters.
Results: From the docking studies, the phytochemical compounds with HMG-CoA reductase inhibition could be classified into 4 groups, including phytosterols, polyphenols, tannins, and flavonoids. Beta-sitosterol exhibited the highest binding affinity to HMG-CoA reductase with a binding energy of -7.75 kcal/mol.
Conclusion: These 10 phytochemical compounds in Triphala potentially exert their cholesterol-lowering effects via inhibition against HMG-CoA reductase. Nonetheless, further *in vitro* and *in vivo* experiments should be conducted subsequently to confirm this finding.

Introduction

Dyslipidemia is a crucial risk factor for atherosclerotic cardiovascular diseases (ASCVDs) and represents the major cause of morbidity and mortality in cardiovascular diseases globally. An elevation of plasma lipids, especially low-density lipoprotein (LDL) and triglyceride (TG), as well as a decrease of plasma high-density lipoprotein (HDL) essentially contribute to the pathogenesis of atherosclerosis (1). When atherosclerosis arises, the arteries become hardened, inflexible, and narrow, and can eventually be blocked if the atherosclerotic plaque ruptures. These pathogenic conditions play a pivotal role in ASCVD progression (2). Therefore, the regulation of

plasma lipid levels is a crucial measure for the prevention and treatment of ASCVD. Lifestyle modifications and pharmacological treatment are both essential strategies currently used for the management of dyslipidemia. In recent decades, antidyslipidemic drugs with various mechanisms of action have been developed. The inhibition against HMG-CoA reductase is one of the effective approaches to reduce plasma LDL levels via a blockade of endogenous cholesterol synthesis in the liver (3). HMG-CoA reductase inhibitors or statins, such as simvastatin, atorvastatin, rosuvastatin, and pitavastatin, have been extensively prescribed as the first-line antidyslipidemic drugs and for the prevention of ASCVD (4). However,

---

***Corresponding author**: Chawannuch Mudjupa,
Email: chawannuch.m@msu.ac.th

considerable shortcomings can frequently ensue during the use of statins, including compelling adverse drug reactions and drug interactions. Various cytochrome P450 (CYP) inhibitors, especially CYP3A4 and 2C9 inhibitors, can substantially increase the plasma levels of certain statins and subsequently cause significant adverse drug reactions. The investigation for an effective HMG-CoA reductase inhibitor with a lower risk of these undesired effects is thus still required. Natural products are considered reservoirs for screening therapeutic agents. Various plant-derived extracts or phytochemicals have been documented as high-potential candidates for antidyslipidemic drug development. Triphala, a well-recognized Ayurvedic formulation, consists of three fruits, *Phyllanthus emblica* L. (Phyllanthaceae), *Terminalia bellirica* (Gaertn.) Roxb. (Combretaceae) and *T. chebula* Retz. (5). The major phytoconstituents of Triphala are gallic acid, ellagic acid, chebulagic acid, chebulinic acid, and corilagin (6). In the experimentally-induced hypercholesterolemia rat model, Triphala supplementation at the doses of 1 g/kg/d for 48 days exhibited significantly lower plasma levels of total cholesterol, TG, free fatty acid, LDL, and VLDL (7). The HMG-CoA reductase inhibition has been proposed as one of the antidyslipidemic mechanisms of action of Triphala (8). The HMG-CoA reductase arranges as a tetramer structure and has four active sites formed by residues of two monomers (9). The active site of HMG-CoA reductase is characterized by the presence of *cis*-loop that fold over part of the HMG-binding pocket (9). Nowadays the interaction between HMG-CoA reductase and statin drugs have been clearly established. However, the binding of promising phytochemicals to the active site of HMG-CoA reductase is still less well examined. In this *in silico* study, the chemical structures of phytoconstituents derived from Triphala formulation were investigated in orientation and binding with HMG-CoA reductase protein by using AutoDock 4.2 program (The Scripps Research Institute, USA) (10). The HMG-CoA reductase inhibitory activities of 10 phytochemical compounds found in Triphala were subsequently ranked according to their binding energy parameters.

Materials and Methods

The tertiary structure of HMG-CoA reductase was obtained from RCSB (Protein Data Bank). For the HMG-CoA reductase protein, the complex between the catalytic portion of human HMG-CoA reductase and atorvastatin (PDB entry code: 1HWK) was used (9). The ligand (atorvastatin) and water were removed by EditPlus Text Editor. The 2D and 3D structures of all ligands (10 phytoconstituents) were sketched and cleaned up by ChemBioDraw Ultra. The prepared 10 ligands were docked to HMG-CoA reductase template. The docking experiments were performed with AutoDock 4.2 (The Scripps Research Institute, USA) (10). The figures were generated using PyMOL software.

Preparation and validation of HMG-CoA reductase template

The X-ray crystallographic structure of human HMG-CoA reductase (PDB entry code: 1HWK) (9) bound to the inhibitor atorvastatin, downloaded from RCSB (Protein Data Bank), was selected for the preparation of HMG-CoA template. The bound crystal was solved by X-ray crystallography techniques with the resolution of 2.22 Å. To prepare the protein template, ligand and water were firstly removed from the protein structure by EditPlus Text Editor Version 3.51. Hydrogens and Gasteiger charges were added to the protein template 1HWK, by using AutoDockTools 1.5.4 (ADT). During the final preparations, nonpolar hydrogens were merged. The 3-dimension (3D) grid was generated by the AutoGrid algorithm to evaluate the binding energies between inhibitor and enzyme. Grid maps for each atom type in the ligands (A, C, HD, N, NA, OA, SA, F, S, Cl) were set and calculated with AutoGrid 4. The affinity and electrostatic potential grid were calculated for each type of atom in the inhibitor. The energies of a particular inhibitor configuration were also calculated. Grid map parameters were set as follows: numbers of points in x-, y- and z-directions were $38 \times 24 \times 38$ with 0.375 Å spacing; center of grid box in x-, y- and z-dimension were $19.34 \times 7.605 \times 15.428$, and these grid map parameters were served for HMG-CoA reductase template validation and docking experiment. The constructed 1HWK template was validated by docking with its crystal ligand, atorvastatin, and other HMG-CoA reductase inhibitors, which bound crystal structures were available.

The chosen crystallographic structures of HMGR, PDB entry codes: 1HWL (9) was superimposed with that of PDB entry code: 1HWK by using Swiss-PDBViewer in order to set the coordinates of the structure. The Iterative Magic Fit function in Swiss-PDBViewer was used to fit and align the molecule in order to examine which amino acid was or was not aligned with each other. Additionally, the misalignment of the amino acids could also be visualized clearly. The constructed HMGR template derived from PDB: 1HWK was set as the reference molecule, then HMGR from 1HWL was selected for superimposition by using the Iterative Magic Fit function, and only alpha carbons were checked. Finally, the new alignment of the 1HWL template was created and the comparative with coordination of 1HWK template and RMSD was reported after imposition in the angstrom unit. Subsequently, the crystal ligand of atorvastatin and the extracted crystal ligands of rosuvastatin (9) from the corresponding PDB entry codes: 1HWK and 1HWL respectively were docked into the active binding pocket of the prepared template (1HWK). The conformations of these ligands obtained from docking or docked poses were compared with the

corresponding crystallographic poses.

Ligand preparation

The 2D structures of all ligands were sketched and cleaned up by ChemBioDraw Ultra, then converted to the corresponding 3D structures by ChemBio3D Ultra. Each 3D structure was cleaned up and the energy was minimized by MM2 in ChemBio3D Ultra before being saved as a mole2 file. The hydrogen atoms were added to each mole2 file of ligand, then the non-polar hydrogen atoms were merged before assigned charges by the Gasteiger-Hückel method in ADT-1.5.6 and saved as pdb file. Next, the aromatic carbons were identified, then rigid root and rotatable bonds were defined in ADT-1.5.6 before saving as a pdbqt file of each ligand.

Docking procedures

The prepared 10 ligands were docked to the HMG-CoA reductase template. The docking experiments were performed with AutoDock 4.2 (The Scripps Research Institute, USA) (10). The prepared ligands were docked to the template by using a Lamarckian genetic algorithm (LGA) for the ligand conformational search. Other docking parameters were set as follows: number of genetic algorithm (GA) runs "100", population size "150", the maximum number of evaluations "15000000", and the maximum number of generations "27000". The final docked conformations were clustered using a tolerance of 2Å root-mean-square deviations (RMSD). Each cluster consisted of conformers, which had similar 3D structures (RMSD <2 Å). The orientation with the lowest docking energy in the cluster of the highest number of members was considered the most stable conformation.

Candidates/phytoconstituents of Triphala

Ten phytoconstituents, which have been documented as the major phytochemicals derived from Triphala were purposely selected to be examined in the HMG-CoA reductase docking study. The list of these phytoconstituents and their natural plant sources are shown in Table 1.

Results

Molecular docking is a tool for studying the binding interaction between macromolecules or target proteins and small molecules. AutoDock 4.2 was used as a tool for investigating the orientation and binding energies in the 10 major phytochemical compounds of Triphala with the active binding site of HMG-CoA reductase. Initially, the HMG-CoA reductase template (PDB code: 1HWK) was validated by docking with its crystal ligand and rosuvastatin (PDB code: 1HWL). Subsequently, 10 phytoconstituents of Triphala were docked into the active binding site of the validated HMG-CoA reductase template. The active compounds were subsequently ranked by the binding energy (ΔG) obtained from the docking analysis for selection. Other essential parameters were also included in the selection i.e., ligand efficacy (LE), number of hydrogen bonds, % conformation, and amino acid residues.

Preparation and validation of HMG-CoA reductase template

The crystal structure of the HMG-CoA reductase template (PDB code: 1HWK) bound with the inhibitor 117 (atorvastatin), solved by the X-ray diffraction technique with the resolution of 2.22 Å. The HMG-CoA reductase template was selected as the prepared template and validated by re-docking the removed crystal ligand, atorvastatin, back into the binding pocket of the prepared template. The validation result of re-docking 117 (atorvastatin) gave the RMSD between docked pose and crystal pose of 0.52 Å. For cross-validation with FBI (rosuvastatin), the RMSD between the docked pose and its corresponding crystal pose was found to be 0.84 Å with a binding energy of -8.15 Kcal/mol. From the validation results, the HMG-CoA reductase-prepared template was a good model and suitable for the docking experiment as shown in Figure 1.

Table 1. Ten major phytoconstituents of Triphala

| Phytoconstituents | Herbal sources | | | Phytochemical classifications | References |
	T. chebula	T. bellirica	P. emblica		
Beta-sitosterol	√			Sterols	(12-14)
Chebulanin	√		√	Tannins	(15-17)
Gallic acid			√	Polyphenols	(11,12,14,18)
Ellagic acid	√	√	√	Polyphenols	(11-14,18)
Corilagin	√	√		Tannins	(11,14,18-20)
Luteolin	√			Flavonoids	(13,14,21)
Quercetin	√	√		Flavonoids	(11,13,14,16,18,21)
Chebulic acid	√			Polyphenols	(11-13,16,21)
Chebulinic acid	√			Tannins	(11,12,15,16,18,21)
Chebulagic acid	√	√		Tannins	(11,14,16,18,20)
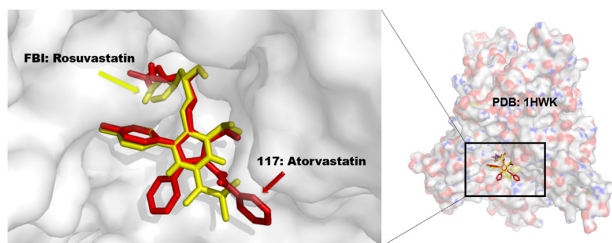
Figure 1. Superimposition between docked pose (yellow) and the corresponding crystallographic pose (red) in the active binding site of HMG-CoA reductase template derived from PDB: 1HWK. The figure was generated using PyMOL software.

Docking study of the phytoconstituents of Triphala

The chemical structures of 10 phytoconstituents of Triphala were docked into the prepared HMG-CoA reductase template. The binding affinity was characterized by binding energy value. The active compounds ranked by the binding energy were listed in Table 2.

The 10 phytoconstituents of Triphala were classified by their chemical structures into four groups, including phytosterols, tannins, polyphenols, and flavonoids. Among 10 phytoconstituents of Triphala, beta-sitosterol from *T. chebula* (13) exhibited the highest binding free energy (ΔG <-7.50 kcal/mol) with two hydrogen bond interactions. The LE was lower than -0.25 (-0.26) and membership in the highest cluster was 42% (Table 2). From the structure of beta-sitosterol, a phenanthrene ring with a beta hydroxy group at C-3 of beta-sitosterol was found to be located in the HMG-binding pocket of HMG-CoA reductase and interacted with Arg590 and Ser684 amino acid residues. Meanwhile, the branched hydrocarbon side chain at C-17 of beta-sitosterol was pointed out from the HMG-binding pocket and bound with a hydrophobic pocket of HMG-CoA reductase (Figure 2A). The beta hydroxy group of beta-sitosterol was found to be located in the HMG-binding pocket at the same position as that of the hydroxy-acid part (HMG-like moiety) of atorvastatin, a synthetic type 2 HMG-CoA reductase inhibitor (22). Additionally, the hydrophobic pocket of HMG-CoA reductase was occupied by the branched hydrocarbon side chain at C-17 of beta-sitosterol which was similar to a large fluorophenyl group of atorvastatin (Figure 2C) (22).

Discussion

From the docking result, beta-sitosterol showed the highest affinity with HMG-CoA reductase. However, its orientation was fit in the hydrophobic pocket due to the flexible structure of the four fused sterol rings. The proper fit between beta-sitosterol and HMG-CoA reductase led to strong hydrophobic interactions. When compared with the conformation of simvastatin, the beta hydroxy group at C-3 of beta-sitosterol was crucial for binding with HMG-CoA reductase binding pocket. The branched hydrocarbon side chain at C-17 of beta-sitosterol also

essentially interacted with the hydrophobic pocket of HMG-CoA reductase.

Beta-sitosterol, which is the main constituent of *T. chebula*, is an organic compound belonging to the family of phytosterols (12). The chemical structure and functions of plant sterols are similar to those of cholesterol in mammals. They are bioactive components found in vegetable oils, spreads, margarine, bread, cereals, and vegetables. Phytosterols are completely soluble in alcohols, but they are insoluble in water and have a relatively low solubility in oils. A wide range of biological activities of beta-sitosterol has been reported such as anxiolytic, sedative, analgesic, immunomodulation, antimicrobials, anticancer, anti-inflammation, hepatoprotection, protective effect on respiratory diseases, wound healing effect, antioxidant, antidiabetic activity, as well as lipid-lowering effect (23). It was documented that the preparation of beta-sitosterol self-microemulsions possessed a significant plasma lipid-lowering effect in hyperlipidemic mice (24). Administration of sitosterol pastils (2 g three times a day) with the main meals significantly reduced the levels of total cholesterol and LDL in children with heterozygous familial hypercholesterolemia (25). It was reported that the add-on treatment of beta-sitosterol (6 g/day) to lovastatin for 12 weeks significantly reduced the plasma LDL level by an additional of 12.8% to 15.1% in hypercholesterolemic patients (26). However, no significant changes in the other plasma lipid levels, such as HDL and lipoprotein (a) were observed. The plasma LDL concentration was decreased by 29.6 ± 1.3% in the hyperlipidemic patients who consumed a portfolio diet containing high plant sterols (1.0 g/1000 kcal) for 4 weeks (27). Beta-sitosterol supplementation at doses of 12-18 g/day significantly lowered both serum total cholesterol and LDL-C (as beta-lipoprotein lipid) in young men with ASCVD (28).

The cholesterol-lowering effect of beta-sitosterol primarily results from its inhibition against intestinal cholesterol absorption (29-31). The chemical structure of plant sterols including beta-sitosterol is similar to that of cholesterol. Thus, beta-sitosterol can inhibit dietary and endogenous cholesterol intestinal absorption by competitive solubilization in the micelle with cholesterol (32). Beta-sitosterol has been found to inhibit intestinal cholesterol absorption in normal volunteers (32). Beta-sitosterol is also considered to disturb the reabsorption of bile acids in the intestine (33). The study in hamsters demonstrated that beta-sitosterol laurate reduced the plasma cholesterol levels via various mechanisms of action including 1) an increase of cholesterol fecal excretion via downregulation of intestinal Niemann–Pick C1-like 1 (NPC1L1) protein and 2) a decrease of bile acid reabsorption which induces conversion of cholesterol into primary bile acids (34). Nonetheless, the other mechanisms of antidyslipidemic action of beta-sitosterol, especially HMG CoA reductase inhibition, have been less

Table 2. Docking studies of HMG-CoA reductase inhibitors and 10 phytoconstituents of Triphala with the catalytic portion of human HMG-CoA reductase

Phytoconstituents of Triphala	Phytochemical groups	Herbal sources	Binding energy (ΔG) Kcal/mol	Ligand efficacy (LE)	Number of H-bond	% Conformation	Amino acid residues
Beta-sitosterol	Sterols	*Terminalia chebula*	-7.75	-0.26	2	42	Arg590, Ser684
Chebulanin	Tannins	*T. chebula, Phyllanthus emblica*	-7.14	-0.16	13	38	Glu559, Gly560 , Ser565, Arg590, Asn658, Ser661, Ser684, Lys691, Lys692, Asn755
Gallic acid	Polyphenols	*P. emblica*	-6.54	-0.55	5	48	Arg590, Ser684, Lys691, Lys735, Asn755
Ellagic acid	Polyphenols	*T. chebula, T. bellirica, P. emblica*	-6.23	-0.28	6	33	Ser684, Lys691, Lys692, Lys735, Ala751, Asn755
Corilagin	Tannins	*T. chebula, T. bellirica*	-6.19	-0.14	11	45	Gly560, Cys561, Arg590, Ser661, Asp690, Lys735, Asn755
Luteolin	Flavonoids	*T. chebula*	-6.18	-0.29	4	70	Gly560, Ser684, Lys692
Quercetin	Flavonoids	*T. chebula, T. bellirica*	-6.01	-0.27	4	52	Gly560, Ser684, Lys692
Chebulic acid	Polyphenols	*T. chebula*	-5.67	-0.23	6	35	Glu559, Arg590, Ser684, Lys735
Chebulinic acid	Tannins	*T. chebula*	-3.86	-0.06	13	4	Glu559, Gly560, Ser565, Ser661, Lys735, Ala751
Chebulagic acid	Tannins	*T. chebula, T. bellirica*	-1.14	-0.02	10	57	Glu559, Cys561, Ser565, Arg590, Lys691, Asn755
Atorvastatin	HMG-CoA reductase inhibitor	-	-12.09	-0.29	7	80	Glu559, Ser565, Ser684, Lys691, Lys692, Lys735, Ala751, Asn755
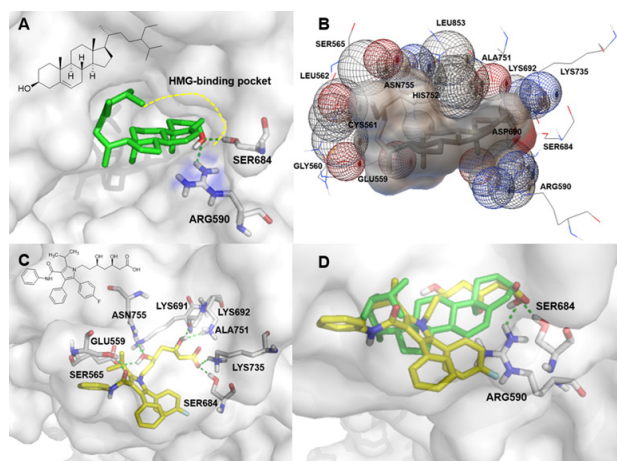
Figure 2. The binding mode of beta-sitosterol and atorvastatin in the binding site of the HMG-CoA reductase template showing (A) two hydrogen bonds of beta-sitosterol in green dashed lines (B) interacted with amino acid residues (C) seven hydrogen bonds of atorvastatin in green dashed lines (D) overlay of beta-sitosterol (green) and atorvastatin (yellow) in the active binding site of HMG-CoA reductase. The figures were generated using PyMOL software.

well investigated.

It was demonstrated that beta-sitosterol derived from *Schizonepeta tenuifolia* significantly reduced intracellular levels of triglycerides and cholesterol in L6 cells via AMPK activation (35). The activation of AMPK is known to cause HMG CoA reductase phosphorylation and inactivation (36). It has been reported that beta-sitosterol derived from *Cassia mimosoides* Linn. at the concentration of 125 μg/mL significantly inhibited HMG-CoA reductase activity (37). To the best of our knowledge, this *in silico* study is the first report of HMG-CoA reductase binding mode and configuration of beta-sitosterol. Beta-sitosterol possibly exerts the lipid-lowering effect via multiple modes of action. Beta-sitosterol is thus likely to play a major role in the hypocholesterolemic effect of Triphala formulation.

The pharmacokinetics of beta-sitosterol in healthy volunteers were documented in the study of Duchateau et al (38). The oral bioavailability of beta-sitosterol was relatively very low at 0.41%. Consequently, the development of beta-sitosterol preparation with higher bioavailability is essential for its HMG CoA reductase inhibitory activity to arise. Beta-sitosterol was found to be distributed in various tissues, including adrenal glands, ovaries, brain, testes, and skin, with a volume of distribution (Vd) of 46 L. The metabolism of beta-sitosterol, which resulted in various metabolites, was reported to occur in the liver as well as in other tissues. Beta-sitosterol is mainly excreted in feces (80%) (33). It was shown that beta-sitosterol had rather low inhibitory activity against CYP3A4 and CYP2D6 enzymes with an IC_{50} of approximately 200 g/mL (39). Therefore, the hazardous interactions between beta-sitosterol and CYP3A4-substrate statins, especially simvastatin, are unlikely. This suggests that beta-sitosterol

can potentially be used safely in a combination with statins to produce the plasma cholesterol-lowering effect.

Tannins, chebulanin, corilagin, chebulinic acid, and chebulagic acid contain polyhydroxy groups in their chemical structures with a high molecular weight of 600-960 g/mole. Mostly, hydroxyl groups interacted with amino acid residues in the binding pocket of HMG-CoA reductase. These hydroxyl groups provide the highest number of hydrogen bonding interactions (10-13 hydrogen bonds) which strengthen the binding between these phytochemical compounds and HMG-CoA reductase. These hydrogen bond interactions also essentially contribute to the stability of ligand-HMG-CoA reductase interactions.

Gallic acid, ellagic acid, and chebulic acid are polyphenolics. The structures of these compounds are composed of polyhydroxy groups with a relatively lower molecular weight of 170-370 g/mole when compared to other chemical groups. From the docking results, gallic acid showed the lowest LE and was located in the pocket of HMG-CoA reductase binding site resulting in the interaction with Arg590, Ser684, Lys691, Lys735, and Asn755. Gallic acid showed a high binding affinity with HMG-CoA reductase and also occupied the same amino acid residues as those of atorvastatin. The binding modes of ellagic acid and chebulic acid from the docking study involved the interaction of six hydrogen bonds with Glu559, Ser684, Lys691, Lys692, Lys735, Ala751, and Asn755. From the previous *in vivo* study, pretreatment with rosuvastatin, ellagic acid, and their combination led to a significant improvement in the lipid profile (40). Similar to rosuvastatin, the hypocholesterolemic activity of ellagic acid is mainly mediated via HMG-CoA reductase inhibition (41). Gallic acid at the doses of 15 mg/kg has also been reported to possess protective effects in the heart, liver, and plasma in the rat model of isoproterenol-induced cardiac toxicity (42).

Lutein and quercetin are flavonoids obtained from *T. chebula* and *T. bellirica*. The LE of two flavonoids was similar to that of atorvastatin with a % conformation of more than 50%. The binding mode of lutein and quercetin from the docking study consisted of four hydrogen bonds with Gly560, Ser684, and Lys692.

From the current docking results, it is indicated that each group of the four active compounds exhibited distinct interactions with HMG-CoA reductase. Beta-sitosterol exhibited the highest affinity with HMG-CoA reductase and its lipid-lowering effect was previously well documented. The tannin group, chebulanin, corilagin, chebulinic acid, and chebulagic acid were nicely bound to the active binding site of HMG-CoA reductase through hydrophobic interaction and the binding was stabilized by 10-13 hydrogen bonds. The hydroxyl groups of compounds in the polyphenol group (gallic acid, ellagic acid, and chebulic acid) primarily interacted with the

crucial amino acid residues in the active binding site of HMG-CoA reductase at the same position as that of atorvastatin.

HMG-CoA reductase inhibition of gallic acid and ellagic acid was also reported earlier. The flavonoids, lutein, and quercetin, were bound to the active binding site of HMG-CoA reductase with a high % conformation of 50 - 70%. These phytoconstituents of Triphala are the active component in the Triphala Ayurvedic formulation. This *in silico* study suggested the potential HMG-CoA reductase inhibition of the active phytochemicals derived from Triphala formulation. However, further *in vitro* and *in vivo* experiments regarding the lipid-lowering effects of these phytochemicals should be investigated.

Conclusion

From the current HMG-CoA reductase docking study, several phytochemicals derived from Triphala substantially exhibited the HMG-CoA reductase binding capability. Beta-sitosterol provided the highest binding affinity toward HMG-CoA reductase with a binding energy of -7.75 kcal/mol. These results indicate that the phytoconstituents in Triphala potentially exert their antidyslipidemic effect via HMG-CoA reductase inhibition.

Authors' contribution

All authors designed the study, carried out the study, wrote the manuscript, and revised the manuscript. All authors read and approved the final version of the manuscript.

Conflict of interests

The authors declare no conflict of interest.

Ethical considerations

The authors considered all ethical issues, including duplications, and the manuscript has been checked for plagiarism.

Funding/Support

References

1. Klop B, Elte JW, Cabezas MC. Dyslipidemia in obesity: mechanisms and potential targets. Nutrients. 2013;5(4):1218-40. doi: 10.3390/nu5041218.

2. Kobiyama K, Ley K. Atherosclerosis: a chronic inflammatory disease with an autoimmune component. Circ Res. 2018;123(10):1118-20. doi: 10.1161/circresaha.118.313816.

3. Illingworth DR, Tobert JA. HMG-CoA reductase inhibitors. Adv Protein Chem. 2001;56:77-114. doi: 10.1016/s0065-3233(01)56003-9.

4. Patel KK, Sehgal VS, Kashfi K. Molecular targets of statins and their potential side effects: not all the glitter is gold. Eur J Pharmacol. 2022;922:174906. doi: 10.1016/j.ejphar.2022.174906.

5. Peterson CT, Denniston K, Chopra D. Therapeutic uses of Triphala in ayurvedic medicine. J Altern Complement Med. 2017;23(8):607-14. doi: 10.1089/acm.2017.0083.

6. Sabina EP, Rasool M. An *in vivo* and *in vitro* potential of Indian ayurvedic herbal formulation Triphala on experimental gouty arthritis in mice. Vascul Pharmacol. 2008;48(1):14-20. doi: 10.1016/j.vph.2007.11.001.

7. Saravanan S, Srikumar R, Manikandan S, Jeya Parthasarathy N, Sheela Devi R. Hypolipidemic effect of Triphala in experimentally induced hypercholesteremic rats. Yakugaku Zasshi. 2007;127(2):385-8. doi: 10.1248/yakushi.127.385.

8. Phimarn W, Sungthong B, Itabe H. Effects of Triphala on lipid and glucose profiles and anthropometric parameters: a systematic review. J Evid Based Integr Med. 2021;26:2515690x211011038. doi: 10.1177/2515690x211011038.

9. Istvan ES, Deisenhofer J. Structural mechanism for statin inhibition of HMG-CoA reductase. Science. 2001;292(5519):1160-4. doi: 10.1126/science.1059344.

10. Morris GM, Goodsell DS, Halliday RS, Huey R, Hart WE, Belew RK, et al. Automated docking using a Lamarckian genetic algorithm and an empirical binding free energy function. J Comput Chem. 1998;19(14):1639-62. doi: 10.1002/(sici)1096-987x(19981115)19:14<1639::aid-jcc10>3.0.co;2-b.

11. Wei X, Luo C, He Y, Huang H, Ran F, Liao W, et al. Hepatoprotective effects of different extracts from Triphala against CCl4-induced acute liver injury in mice. Front Pharmacol. 2021;12:664607. doi: 10.3389/fphar.2021.664607.

12. Tarasiuk A, Mosińska P, Fichna J. Triphala: current applications and new perspectives on the treatment of functional gastrointestinal disorders. Chin Med. 2018;13:39. doi: 10.1186/s13020-018-0197-6.

13. Sarkar A, Agarwal R, Bandyopadhyay B. Molecular docking studies of phytochemicals from *Terminalia chebula* for identification of potential multi-target inhibitors of SARS-CoV-2 proteins. J Ayurveda Integr Med. 2022;13(2):100557. doi: 10.1016/j.jaim.2022.100557.

14. Belapurkar P, Goyal P, Tiwari-Barua P. Immunomodulatory effects of Triphala and its individual constituents: a review. Indian J Pharm Sci. 2014;76(6):467-75.

15. Cheng HY, Lin TC, Yu KH, Yang CM, Lin CC. Antioxidant and free radical scavenging activities of *Terminalia chebula*. Biol Pharm Bull. 2003;26(9):1331-

5. doi: 10.1248/bpb.26.1331.

16. Nigam M, Mishra AP, Adhikari-Devkota A, Dirar AI, Hassan MM, Adhikari A, et al. Fruits of *Terminalia chebula* Retz.: a review on traditional uses, bioactive chemical constituents and pharmacological activities. Phytother Res. 2020;34(10):2518-33. doi: 10.1002/ptr.6702.

17. Zhao Y, Liu F, Liu Y, Zhou D, Dai Q, Liu S. Anti-arthritic effect of chebulanin on collagen-induced arthritis in mice. PLoS One. 2015;10(9):e0139052. doi: 10.1371/journal.pone.0139052.

18. Charoenchai L, Pathompak P, Madaka F, Settharaksa S, Saingam W. HPLC-MS profiles and quantitative analysis of Triphala formulation. Bull Health Sci Technol. 2016;14(1):57-67.

19. Duan W, Yu Y, Zhang L. Antiatherogenic effects of *Phyllanthus emblica* associated with corilagin and its analogue. Yakugaku Zasshi. 2005;125(7):587-91. doi: 10.1248/yakushi.125.587.

20. Zhang YJ, Nagao T, Tanaka T, Yang CR, Okabe H, Kouno I. Antiproliferative activity of the main constituents from *Phyllanthus emblica*. Biol Pharm Bull. 2004;27(2):251-5. doi: 10.1248/bpb.27.251.

21. Wang W, Liu T, Yang L, Ma Y, Dou F, Shi L, et al. Study on the multi-targets mechanism of Triphala on cardio-cerebral vascular diseases based on network pharmacology. Biomed Pharmacother. 2019;116:108994. doi: 10.1016/j.biopha.2019.108994.

22. Istvan ES. Structural mechanism for statin inhibition of 3-hydroxy-3-methylglutaryl coenzyme A reductase. Am Heart J. 2002;144(6 Suppl):S27-32. doi: 10.1067/mhj.2002.130300.

23. Babu S, Jayaraman S. An update on β-sitosterol: a potential herbal nutraceutical for diabetic management. Biomed Pharmacother. 2020;131:110702. doi: 10.1016/j.biopha.2020.110702.

24. Yuan C, Zhang X, Long X, Jin J, Jin R. Effect of β-sitosterol self-microemulsion and β-sitosterol ester with linoleic acid on lipid-lowering in hyperlipidemic mice. Lipids Health Dis. 2019;18(1):157. doi: 10.1186/s12944-019-1096-2.

25. Becker M, Staab D, Von Bergmann K. Treatment of severe familial hypercholesterolemia in childhood with sitosterol and sitostanol. J Pediatr. 1993;122(2):292-6. doi: 10.1016/s0022-3476(06)80136-8.

26. Richter WO, Geiss HC, Sönnichsen AC, Schwandt P. Treatment of severe hypercholesterolemia with a combination of beta-sitosterol and lovastatin. Curr Ther Res Clin Exp. 1996;57(7):497-505. doi: 10.1016/s0011-393x(96)80059-2.

27. Jenkins DJ, Kendall CW, Marchie A, Faulkner DA, Wong JM, de Souza R, et al. Direct comparison of a dietary portfolio of cholesterol-lowering foods with a statin in hypercholesterolemic participants. Am J Clin Nutr. 2005;81(2):380-7. doi: 10.1093/ajcn.81.2.380.

28. Gylling H, Plat J, Turley S, Ginsberg HN, Ellegård L, Jessup W, et al. Plant sterols and plant stanols in the management of dyslipidaemia and prevention of cardiovascular disease. Atherosclerosis. 2014;232(2):346-60. doi: 10.1016/j.atherosclerosis.2013.11.043.

29. Miettinen TA, Puska P, Gylling H, Vanhanen H, Vartiainen E. Reduction of serum cholesterol with sitostanol-ester margarine in a mildly hypercholesterolemic population. N Engl J Med. 1995;333(20):1308-12. doi: 10.1056/nejm199511163332002.

30. Ostlund RE Jr. Phytosterols in human nutrition. Annu Rev Nutr. 2002;22:533-49. doi: 10.1146/annurev.nutr.22.020702.075220.

31. Pouteau EB, Monnard IE, Piguet-Welsch C, Groux MJ, Sagalowicz L, Berger A. Non-esterified plant sterols solubilized in low fat milks inhibit cholesterol absorption--a stable isotope double-blind crossover study. Eur J Nutr. 2003;42(3):154-64. doi: 10.1007/s00394-003-0406-6.

32. Heinemann T, Kullak-Ublick GA, Pietruck B, von Bergmann K. Mechanisms of action of plant sterols on inhibition of cholesterol absorption. Comparison of sitosterol and sitostanol. Eur J Clin Pharmacol. 1991;40 Suppl 1:S59-63.

33. Bin Sayeed MS, Karim SMR, Sharmin T, Morshed MM. Critical analysis on characterization, systemic effect, and therapeutic potential of beta-sitosterol: a plant-derived orphan phytosterol. Medicines (Basel). 2016;3(4):29. doi: 10.3390/medicines3040029.

34. Chen S, Wang R, Cheng M, Wei G, Du Y, Fan Y, et al. Serum cholesterol-lowering activity of β-sitosterol laurate is attributed to the reduction of both cholesterol absorption and bile acids reabsorption in hamsters. J Agric Food Chem. 2020;68(37):10003-14. doi: 10.1021/acs.jafc.0c04386.

35. Hwang SL, Kim HN, Jung HH, Kim JE, Choi DK, Hur JM, et al. Beneficial effects of beta-sitosterol on glucose and lipid metabolism in L6 myotube cells are mediated by AMP-activated protein kinase. Biochem Biophys Res Commun. 2008;377(4):1253-8. doi: 10.1016/j.bbrc.2008.10.136.

36. Carling D, Zammit VA, Hardie DG. A common bicyclic protein kinase cascade inactivates the regulatory enzymes of fatty acid and cholesterol biosynthesis. FEBS Lett. 1987;223(2):217-22. doi: 10.1016/0014-5793(87)80292-2.

37. Shen C, Huang L, Xiang H, Deng M, Gao H, Zhu Z, et al. Inhibitory effects on the HMG-CoA reductase in the chemical constituents of the *Cassia mimosoides* Linn. Rev Rom Med Lab. 2016;24(4):413-22. doi: doi:10.1515/rrlm-2016-0041.

38. Duchateau G, Cochrane B, Windebank S, Herudzinska J, Sanghera D, Burian A, et al. Absolute oral bioavailability and metabolic turnover of β-sitosterol in healthy subjects. Drug Metab Dispos.

2012;40(10):2026-30. doi: 10.1124/dmd.112.046623.

39. Vijayakumar TM, Kumar RM, Agrawal A, Dubey GP, Ilango K. Comparative inhibitory potential of selected dietary bioactive polyphenols, phytosterols on CYP3A4 and CYP2D6 with fluorometric high-throughput screening. J Food Sci Technol. 2015;52(7):4537-43. doi: 10.1007/s13197-014-1472-x.

40. Elhemely MA, Omar HA, Ain-Shoka AA, Abd El-Latif HA, Abo-youssef AM, El Sherbiny GA. Rosuvastatin and ellagic acid protect against isoproterenol-induced myocardial infarction in hyperlipidemic rats. Beni Suef Univ J Basic Appl Sci. 2014;3(4):239-46. doi: 10.1016/j.bjbas.2014.10.010.

41. Kannan MM, Quine SD. Ellagic acid inhibits cardiac arrhythmias, hypertrophy and hyperlipidaemia during myocardial infarction in rats. Metabolism. 2013;62(1):52-61. doi: 10.1016/j.metabol.2012.06.003.

42. Shaik AH, Shaik SR, Daddam JR, Ali D, Manoharadas S, Arafah MW, et al. Maslinic acid and gallic acid protective efficacy on lipids, lipoproteins and lipid metabolizing enzymes against isoproterenol administered cardiotoxicity: an *in vivo* and *in silico* molecular docking evidences. J King Saud Univ Sci. 2021;33(1):101230. doi: 10.1016/j.jksus.2020.101230.